

In-Situ TEM Monitoring of Thermal Decomposition in Individual Boron Nitride Nanotubes

Hessam M. Ghassemi, Chee H. Lee, Yoke K. Yap, and Reza S. Yassar

The future of microelectronic and nanoelectronics devices could lie in one-dimensional nanomaterials including boron nitride nanotubes (BNNTs). In such applications, however, the flow of electrical current may induce structural failure resulting in reduction of component service life. Here, we utilized scanning tunneling microscopy inside a transmission electron microscope to study the thermal failure of individual multi-walled BNNTs via Joule heating. At elevated temperatures, the nanotube failed by the formation of amorphous nanoclusters and progression of structural defects. These clusters have various sizes and initially form on the outermost shell layers of BNNTs.

INTRODUCTION

Boron nitride nanotubes (BNNTs) are structurally similar to carbon nanotubes (CNTs), where alternating boron and nitrogen form an ionic structure. Their mechanical properties are predicted to be similar to carbon nanotubes.¹ The Young's modulus of BNNTs have been reported in the range of 0.5–0.8 Tpa.^{2–4} These nanotubes are also insulators due to their wide band gap of 5.4 eV or higher.⁵ Thermal characterization of BNNTs showed better stability at higher temperatures in comparison to CNTs. Thermogravimetry curves indicated that BNNTs started to decompose at 950°C, while in the case of CNTs oxidation happened at 500°C.⁶ Thus BNNTs are prospective wide band gap semiconductors for high-power, high-temperature devices.

The study of material failure at elevated temperatures is important for high-temperature applications of new energy technologies and electronic systems.^{7,8} In the case of nanotubes and nanowires, one can study the thermal

stability and failure of such structures using the Joule heating method.^{9–12} According to this approach, at the presence of electrical current, the nanowire or nanotube can be heated to high temperatures. This can result in the variation of electrical properties. Moreover, at elevated temperatures, phase transformation may be induced, and decomposition of the structure may be observed.

While there are a number of reports on mechanical properties of BNNTs at room temperatures,^{3,13,14} the failure of BNNTs has rarely been studied at high temperatures.¹⁰ In this paper, we report the real-time thermal decomposition of individual BNNTs by the use of an in situ scanning tunneling microscope

(STM) inside a transmission electron microscope (TEM). Individual samples were kept under high constant bias voltage of 100 V while TEM images were recorded in situ to capture the decomposition process.

See the sidebar for experimental procedures.

RESULTS AND DISCUSSION

Individual BNNTs were connected to the STM tip at one end and the Au wire on the other end. Before Joule heating, the outer diameters of the nanotubes were measured to be ~50 nm, while their lengths averaged ~1 μm (Figure 1a and b). Average inner shell distance was ~0.35 nm (Figure 1c). The structures of the tested nanotubes had no amorphous layer on the outer shells.

Individual nanotubes were then subjected to a bias voltage according to the design shown in Figure A. The electrical current, I , as a function of applied bias voltage, V , was monitored for each nanotube as shown in Figure 2a. More than 50 different BNNTs were examined and the recorded I - V data showed consistency. Negligible current could be detected even at high bias voltages. This confirms an insulator behavior in the BNNTs. This is expected, as our BNNTs possess a wide energy band gap.¹⁷ As shown in Figure 2b, the strong absorption in UV-visible spectroscopy corresponds to the optical band gap of 5.9 eV, which is higher than the values reported by others by the magnitude of 0.4 eV.^{15,17} The absorption band at ~4.75 eV is due to the intrinsic dark exciton absorption. We suggest that the relatively small absorption at ~3.7 eV may be associated with defects in the BNNTs.¹⁷

One should note that the contact resistance can not be the reason for negli-

How would you...

...describe the overall significance of this paper?

Here we have shown that the structure of ionic type tubes can be collapsed due to the application of electrical voltage and transport of small amounts of electrical current. This new understanding will help materials scientists to better evaluate the reliability of nanoelectronic devices.

...describe this work to a materials science and engineering professional with no experience in your technical specialty?

The size of electronic devices becomes smaller and smaller and the utilized components and materials are subjected to complex environments including high temperatures, electrical current, mechanical stresses, and others. We need to evaluate the performance of these small-scale materials that are used in such devices. We have shown that these small-scale materials may suffer structural degradation under such environments.

EXPERIMENTAL PROCEDURES

The synthesis of boron nitride nanotubes (BNNTs) is challenging and requires very high growth temperatures ($>1,500^{\circ}\text{C}$), a specific fabrication system, or dangerous chemistry.^{15,16} Recently, we have succeeded in growing BNNTs without dangerous chemicals in a conventional tube furnace.¹⁷ These BNNTs can be grown directly on Si substrates by thermal chemical vapor deposition at $1,100\text{--}1,200^{\circ}\text{C}$. Ultraviolet-visible absorption spectroscopy (HP 8453 Spectrophotometer) was also used to further characterize the as-grown BNNTs. This was performed by a suspension of BNNTs in ethanol. These multi-walled BNNTs were used in Joule heating experiments. These experiments were conducted inside the chamber of a JEOL JEM-4000FX transmission electron microscope (TEM) operating at 200 Kv using an in situ scanning tunneling microscope (STM) holder. The schematic of this holder is shown in Figure Aa. It consists of a sapphire ball and a piezo tube mounted on Au wire, which can approach the STM tip. Figure Ab represents the whole electric circuit when STM tip, BNNTs and Au wire are connected.

Individual BNNTs were then attached to an Au wire either through mechanical scratching of the wire on the Si substrate or using silver paint. Then the wire was fixed on a hat which fits on top of a sapphire ball, connected to stacks of piezoelectric layers that allow nanometer motion of the sample toward the STM tip. Using the Nanofactory™ software (NFC3), each sample position was adjusted with a precision of 1 nm in X, Y, and Z directions.³ Here, the samples were always grounded, and bias voltage was applied to the tungsten STM tip. The STM tip was then inserted into each nanotube to assure a stable contact (Figure B). Constant bias voltage of 100 V was applied to the samples while the current flows were captured as a function of time. To eliminate the possibility for the promotion of thermal decomposing via the electron beam, the experiments were conducted at low intensity electron beam. Also, the accelerating voltage was reduced from 300 Kv to 200 Kv.

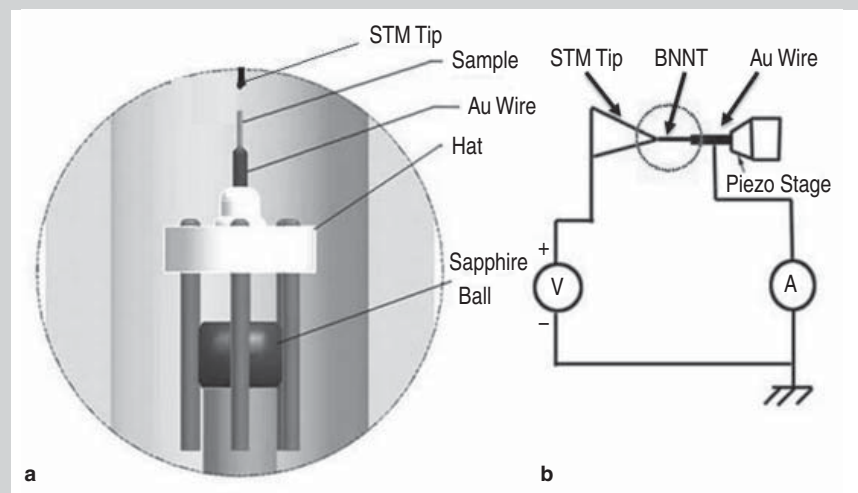


Figure A. (a) A schematic of the utilized STM-TEM sample holder. Sample mounted on Au wire approaches the STM tip via sliding on the sapphire ball. (b) The electric circuit as the BNNT is connected to the STM tip and Au wire.

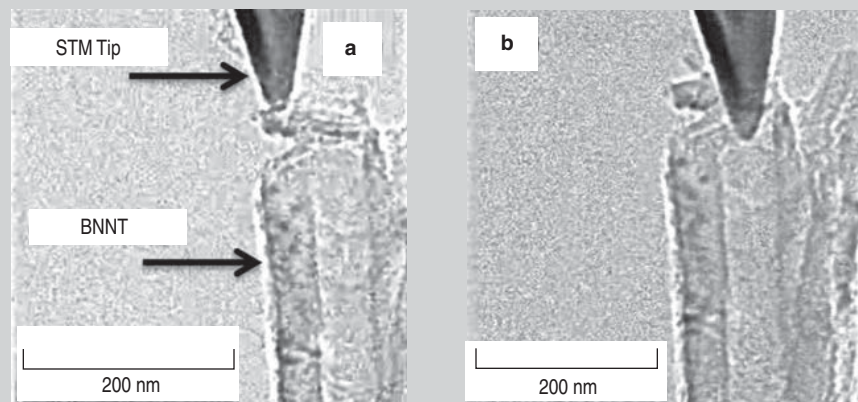


Figure B. (a, b) TEM images correspond to the process of inserting the STM tip into the nanotube to secure the electrical contact.

gible conductivity in the tested BNNTs. These nanotubes are proven to be insulators by previously published articles (e.g. References 5, 6, 10, 14–18) due to their large band gap. In addition, we have tested several other nanotubes and nanowires (ZnO, TiO_2 , VN, C) and the amount of detected current is in accordance with their expected electrical behavior.

In the Joule heating technique, a number of samples were subjected to high bias voltages that led to current flow through the individual nanotubes. Considering that the input power depends on the square root of current, one expects a high amount of thermal energy to be released due to electron transport in the nanotube. Part of this thermal energy is transferred to the vacuum and the rest increases the temperature of the nanotube. Previous Joule heating experiments estimated the temperature to be more than $1,900^{\circ}\text{C}$.¹⁰ Figure 3 shows the Joule heating current versus time after the application of 100 V bias on a nanotube. The detected current increases slightly in the beginning and increases more rapidly after 77 seconds. This is then followed by a sudden drop of current at 95 seconds. The abrupt drop in current, shown in Figure 3, corresponds to the structural failure of the nanotube that results in the disconnection of the STM-BNNT-wire electrical circuit. Inset of Figure 3 shows the broken part of the nanotube attached to the STM tip after failure.

Figure 4 a–f represents the TEM snapshots of thermal decomposition of a BNNT under the application of 100 V bias voltage. One can notice the formation and enlargement of nanoclusters (shown by black arrows) during the decomposition process. The formation of the clusters was faster than the video rate of our camera and thus the capture of initial stage of clustering was quite difficult. No crystallinity could be observed during high resolution TEM analysis, which suggests amorphous structures for these nanoparticles. This finding is in agreement with a recent report.¹⁰ Electron energy loss spectroscopy analysis, performed by Zhi et al.,¹⁰ suggests that these particles are clusters of boron atoms. In our case, it is possible that some elements from the STM electrode be inserted into these

clusters as the clusters appear to have higher contrast in comparison to the nanotubes. The nitrogen atoms likely leave the structure in the vacuum due to high temperature heating and the application of bias voltage. This bias voltage further strengthens the driving force for the dissociation of bonds in ionic BN structures. Temperatures up to 1,900°C have been reported depending on the geometry of the nanotube.^{9,10}

From Figure 4, one can see that the decomposition process initiates at the outermost shell layers. This is evident by monitoring the formation of voids on the external shells shown by gray arrows in Figure 4b–f. While the inner shells remain almost intact, the depth of voids in outer shells gradually increases. Our finding is opposite to the recent report of Zhi et al.¹⁰ that reported the start of decomposition process from inner shells. As the gray arrows indicate, the voids become deeper while the size of adjacent nanoparticles increases (follow the black arrows in (c) through (f)). These changes suggest that the outer shells of our BNNTs most likely have relatively higher defect density in comparison to inner shells. In addition, structural defects can act as initial sites of decomposition events. Point defects such as vacancy defects turn the favorite B–N bonds to B–B or N–N. As such, the honeycomb morphology converts to 7-5-5-7 defect (Stone–Wales).¹⁹ These defects have large thermodynamic energies and a higher tendency to evolve upon heating and initiating the decomposition process.

It is worth mentioning that nanoparticles formed at different sizes along the length of the nanotube. More particles could be detected (Figure 5a) in the vicinity of the STM tip while fewer particles could be observed in the areas far from the tip (Figure 5b and c). One reason for this could be defect density which gives rise to the decomposing at one end of nanotube, even though the theoretical calculations²⁰ predicted that the center of the nanotube should have higher temperature in comparison to the ends. One should note that the assumptions in Reference 20 may not be applicable to our experimental analysis. Some of these assumptions are (a) the current density in the contacts is three orders of magnitude smaller than in

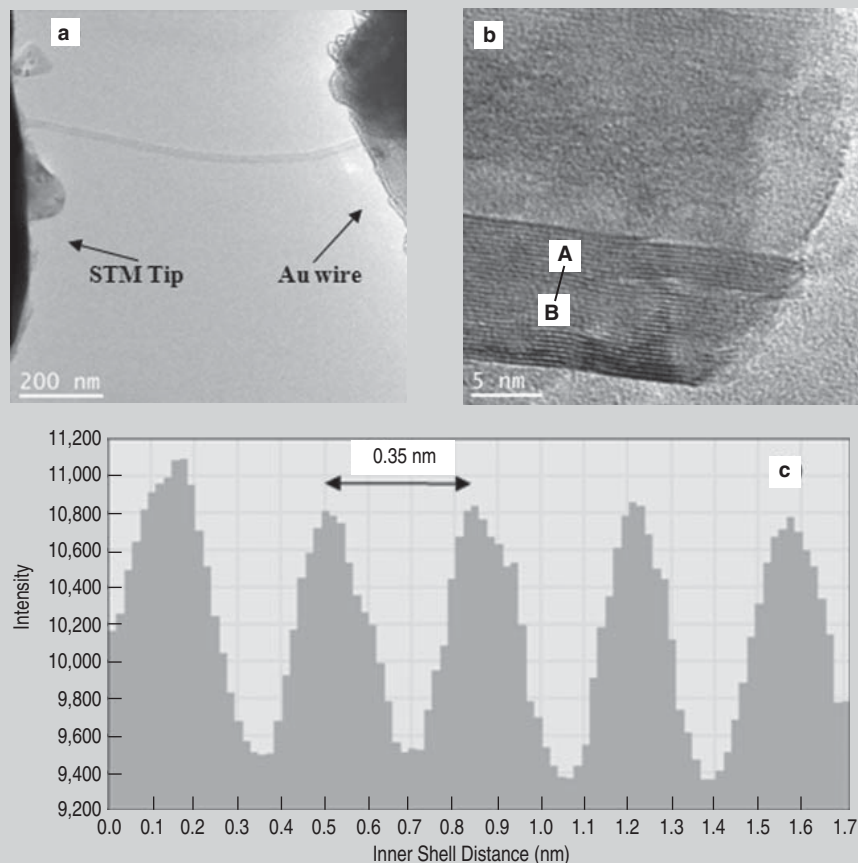


Figure 1. (a) A TEM image of a BNNT connected across the Au wire and the STM tip. (b) High resolution TEM image of the end of an individual BNNT shows that there is no amorphous layer or contamination outside or inside the nanotube. (c) The inner-shell distances of a BNNT is determined as 0.35 nm, based on the intensity histogram obtained along the AB line in (b).

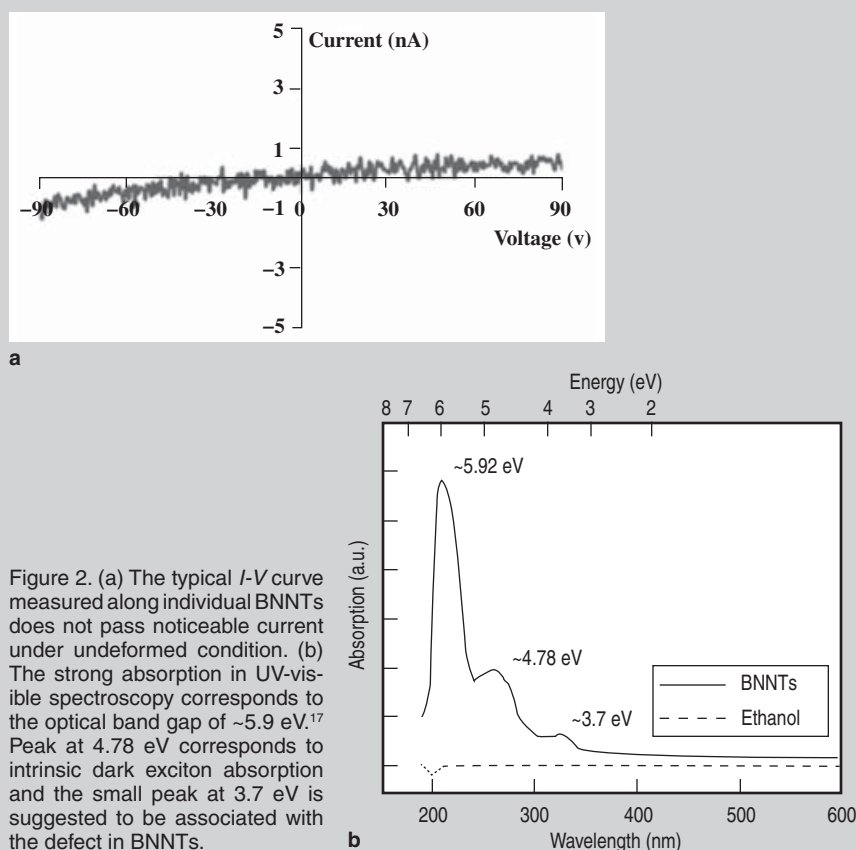


Figure 2. (a) The typical *I*-*V* curve measured along individual BNNTs does not pass noticeable current under undeformed condition. (b) The strong absorption in UV-visible spectroscopy corresponds to the optical band gap of ~5.9 eV.¹⁷ Peak at 4.78 eV corresponds to intrinsic dark exciton absorption and the small peak at 3.7 eV is suggested to be associated with the defect in BNNTs.

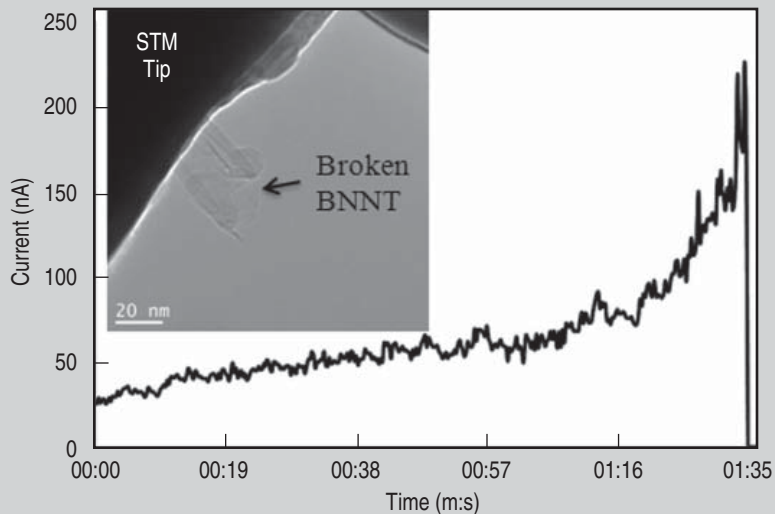


Figure 3. Current flow as a function of duration of applied voltage. Constant voltage of 100 V was applied to an individual nanotube. Current increases slightly in the beginning and increases more rapidly after 77 seconds. The sudden drop of current at 95 seconds corresponds to the disconnection of STM-BNNT-wire circuit due to the BNNT decomposition. (Inset) TEM image showing the broken nanotube is attached to the STM tip.

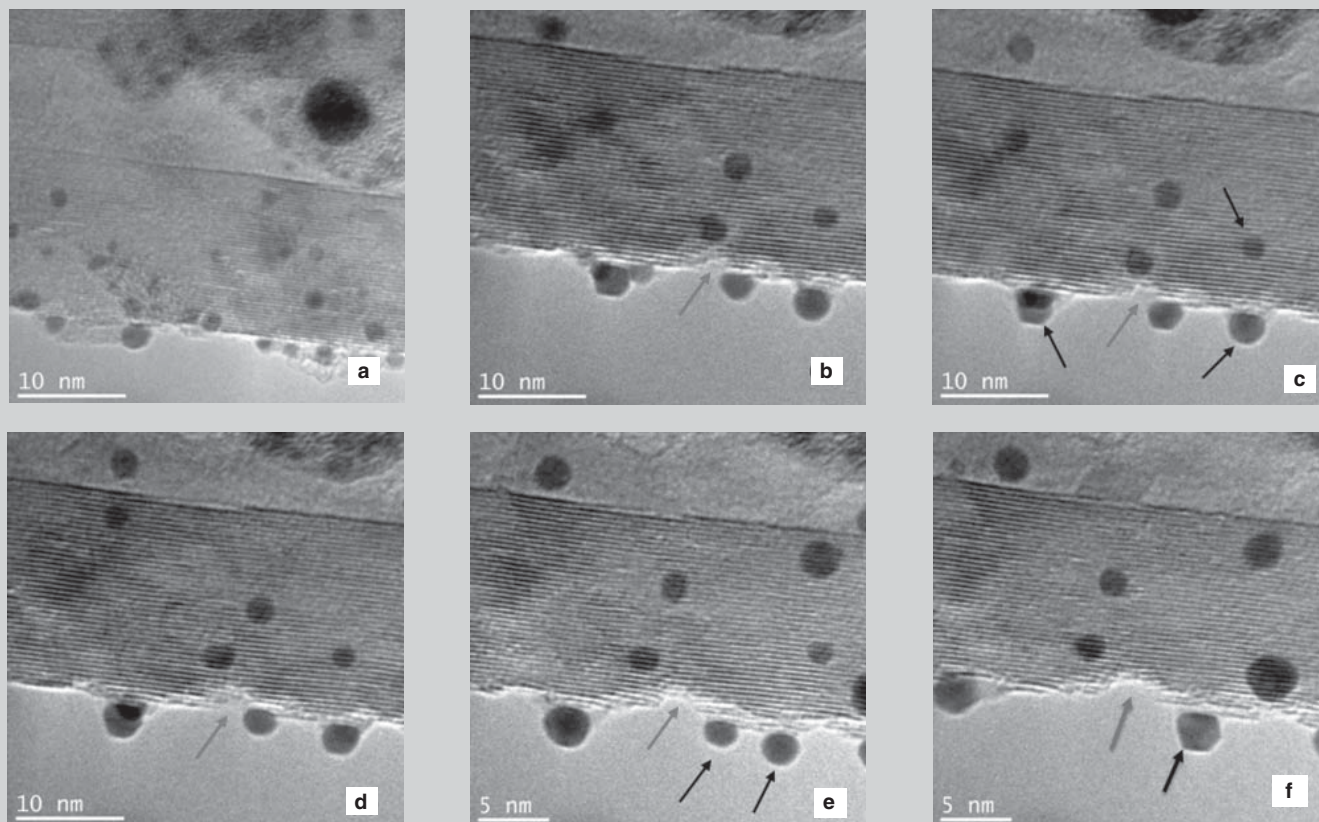


Figure 4. (a–f) High-resolution TEM images correspond to the process of nanoparticles formation during the thermal decomposition of BN nanotubes. Black arrows points toward the growth of nanoparticles on the outermost shell layers. Gray arrows indicate the void formation in the outer shell of the BN nanotube and its propagation toward the inner shells.

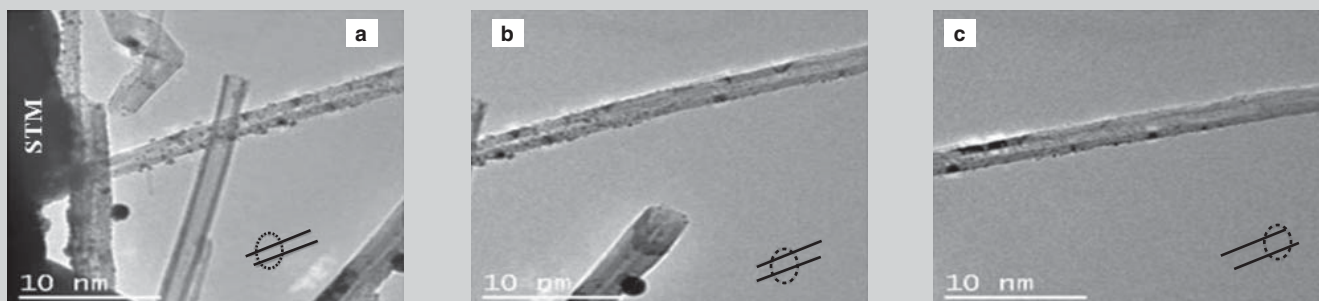


Figure 5. TEM images show variations in the density of nanoparticles during the thermal decomposition of a BN nanotube. Regions near the STM tip (a) with more particles indicate higher temperatures compared to zones further away from the STM tip (b and c). The locations of these TEM images are taken from different parts of the BNNT as schematically drawn in these images.

the wire, and the heat generation term within the contacts is neglected. This assumption cannot be the case in our experiments. (b) The current density is described by a step function, which might not be the case here. In our case, there are Schottky barriers at contact points, causing non-linearity in the I - V curves.¹⁸ (c) There are no “hot spots” within the wire, i.e., localized points of higher resistance than the surroundings, which also may not be true in our case due to structural/defect variation in the nanotubes.

One should note that the decomposition of BNNTs can not be due to electron beam exposure. If this was the case, then such decomposition phenomenon should also be seen during normal TEM imaging of BNNTs. But, in fact the formation of clusters was observed only when the bias voltage was applied. In addition, the exposure to electron beam damage was minimized by expanding the beam over the entire screening area and the accelerating voltage was decreased from 300 to 200 Kv.

CONCLUSION

Thermal decomposition of individual BNNTs was studied via in situ TEM imaging. Real-time monitoring shows that, with the Joule heating experiment, the BN nanotubes fail through the dissociation of atomic structure resulting in the formation of nanoparticles with different sizes and population density. These particles form mostly on outer shell layers, and the presence of structural defects may act as the active site of dissociation event. Such information is invaluable for designing robust nanotube-based electronic circuits subjected to current flow.

ACKNOWLEDGEMENT

R.S. Yassar and Y.K. Yap acknowledge National Science Foundation (NSF)-DMR grant no. 0820884 and NSF-CMMI grant no. 0926819. R.S.Y acknowledges the support from Michigan Space Grant Consortium (Grant no. 2000433 MSGC). Y.K.Y acknowledges his NSF CAREER award (Award no. 0447555) and the U.S. Department of Energy, the Office of Basic Energy Sciences (Grant No. DE-FG02-06ER46294) for supporting the efforts

on the synthesis of boron nitride nanotubes.

References

1. V. Verma, V.K. Jindal, and K. Dharamvir, “Elastic Moduli of a Boron Nitride Nanotube,” *Nanotechnology*, 18 (2007), pp. 435711–435717.
2. D. Golberg et al., “Direct Force Measurements and Kinking under Elastic Deformation of Individual Multiwalled Boron Nitride Nanotubes,” *Nano Letters*, 7 (2007), pp. 2146–2151.
3. H. Ghassemi, Y.K. Yap, and R.S. Yassar, “In-situ Nanomechanical Testing of One-dimensional Materials,” *Proceeding of Nanotech 2009* (Cambridge, MA: Nano Science & Technology Institute, 2009), pp. 318–322.
4. A.P. Suryavanshi et al., “Elastic Modulus and Resonance Behavior of Boron Nitride Nanotubes,” *Applied Physics Letters*, 84 (2004), pp. 2527–2529.
5. X. Blasé et al., “Stability and Band Gap Constancy of Boron Nitride Nanotubes,” *Europhysics Letters*, 28 (1994), pp. 335–340.
6. D. Golberg et al., “Synthesis and Characterization of Ropes Made of BN Multiwalled Nanotubes,” *Scripta Materialia*, 44 (2001), pp. 1561–1565.
7. Y.K. Kwon, D. Tomanek, and S. Iijima, “‘Bucky Shuttle’ Memory Device: Synthetic Approach and Molecular Dynamics Simulations,” *Physical Review Letters*, 82 (1999), pp. 1470–1473.
8. P.G. Collins et al., “Nanotube Nanodevice,” *Science*, 278 (1997), pp. 100–102.
9. J.Y. Huang et al., “Real-Time Observation of Tubule Formation from Amorphous Carbon Nanowires under High-Bias Joule Heating,” *Nano Letters*, 6 (2007), pp. 1699–1705.
10. X. Zhi, D. Golberg, and Y. Bando, “In situ TEM-STM Recorded Kinetics of Boron Nitride Nanotube Failure under Current Flow,” *Nano Letters*, 9 (2009), pp. 2251–2254.
11. J.Y. Huang, F. Ding, and B.I. Yakobson, “Dislocation Dynamics in Multiwalled Carbon Nanotubes at High Temperatures,” *Physical Review Letters*, 100 (2008), pp. 035503–035507.

12. J.Y. Huang et al., “Real Time Microscopy, Kinetics, and Mechanism of Giant Fullerene Evaporation,” *Physical Review Letters*, 17 (2007), pp. 175503–175507.
13. H. Ghassemi and R.S. Yassar, “On the Mechanical Behavior of Boron Nitride Nanotubes,” *Appl. Mechanics Review*, 63 (2010), pp. 020801-1–020804-7.
14. X. Bai et al., “Deformation-Driven Electrical Transport of Individual Boron Nitride Nanotubes,” *Nano Letters*, 7 (2007), pp. 632–637.
15. J. Wang et al., “Multiwalled Boron Nitride Nanotubes: Growth, Properties, and Applications,” *B-C-N Nanotubes and Related Nanostructures, Lecture Notes in Nanoscale Science and Technology*, ed. Y.K. Yap (New York: Springer, 2009), pp. 23–44.
16. J. Wang et al., “Low Temperature Growth of Boron Nitride Nanotubes on Substrates,” *Nano Letters*, 5 (2005), pp. 2528–2532.
17. C.H. Lee et al., “Effective Growth of Boron Nitride Nanotubes by Thermal Chemical Vapor Deposition,” *Nanotechnology*, 19 (2008), pp. 455605–455610.
18. H. Ghassemi et al., “On the Relation of Mechanical Deformation and Electrical Properties of BN Nanotubes,” *Nanotubes and Related Nanostructures-2009*, ed. Y.K. Yap (Warrendale, PA: MRS, 2009), p. 1204-K17-03.
19. A.J. Stone and D.J. Wales, “Theoretical Studies of Icosahedral C60 and Some Related Species,” *Chemistry Physics Letters*, 128 (1986), pp. 501–503.
20. C. Durkan, M.A. Schneider, and M.E. Welland, “Analysis of Failure Mechanisms in Electrically Stressed Au Nanowires,” *Journal of Applied Physics*, 86 (1999), pp. 1280–1286.

Hessam M. Ghassemi and Reza S. Yassar are with the Department of Mechanical Engineering-Engineering Mechanics, Michigan Technological University, 1400 Townsend Dr., Houghton, MI 49931, USA; Chee H. Lee and Yoke K. Yap are with the Department of Physics, Michigan Technological University, 1400 Townsend Dr., Houghton, MI 49931, USA. Dr. Yassar can be reached at reza@mtu.edu and Dr. Yap can be reached at ykyap@mtu.edu.

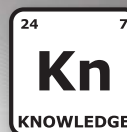
Jim Evans Honorary Symposium

B. Li, B. Thomas, L. Zhang, F. Doyle, A. Campbell, editors

This symposium represents Jim Evans, Professor of Metallurgy Emeritus and the P. Malozemoff Professor Emeritus in the Department of Materials Science and Engineering, University of California, Berkeley, which he joined in 1972. His research deals with rate phenomena governing the productivity of processes for producing metals and other materials. This has involved investigations of wide ranging technologies such as aluminum reduction cells, electromagnetic casters, chemical vapor deposition, fluidized bed electrodes and batteries.

Topics covered included:

- Materials production
- Fluid flow in materials production
- Mass transport in materials production
- Modeling of materials production
- Electrochemical phenomena in materials production
- Electromagnetic phenomena in materials production.
- Sensors and measurement of physical parameters in high temperature and hostile environments
- Control of environmental impact of materials production
- Novel cells for aqueous electrolysis
- Novel cells for molten salt electrolysis
- Mathematical modeling in light metals production
- Novel batteries
- Novel leaching reactors



TMS Member price: 109.00 • Non-member price: 154.00 • TMS Student Member price: 84.00